ELSEVIER

Global and Planetary Change 27 (2000) 39–52

GLOBAL AND PLANETARY CHANGE

www.elsevier.com/locate/gloplacha

Modelling the Middle Pleistocene uplift in the Ardennes–Rhenish Massif: thermo-mechanical weakening under the Eifel?

Daniel Garcia-Castellanos [a,*], Sierd Cloetingh [a], Ronald Van Balen [b]

[a] *Faculty of Earth Sciences, Vrije Universiteit, de Boelelaan, 1085, 1081HV Amsterdam, Netherlands*

[b] *Netherlands Institute of Applied Geosciences TNO / National Geological Survey, P.O. Box 80015, 3508TA Utrecht, Netherlands*

Abstract

Middle Pleistocene uplift in the Eifel has been interpreted as the isostatic response of the lithosphere to a deep buoyant hot body. The spatial and temporal distribution of the uplift in the Ardennes–Rhenish Massif Region has recently been constrained by new data of river incision that have been compiled in this work. The uplift distribution can be reproduced using a thin elastic plate model and assuming that the uplift is created by a deep buoyant load, the distribution of which coincides with the weakening. Models incorporating a lithospheric weakening provide a better fit of the observed uplift than models with homogeneous flexural rigidity. These results are confirmed by numerical experiments using a depth-dependent elasto-plastic plate rheology, linking the flexural model with the thermo-mechanical structure of the lithosphere. © 2000 Elsevier Science B.V. All rights reserved.

Keywords: Ardennes–Rhenish Massif; thermo-mechanical weakening; Eifel

1. Introduction

The Rhenish Massif is part of the Variscan orogenic belt in Northwestern Europe, and is located near the borders between Belgium, France, Luxembourg and Germany (Fig. 2). The Ardennes represent the most western part of the massif. After its formation in Late Palaeozoic times, the Ardennes–Rhenish Massif has remained a permanent high affected by uplift and denudation. At present, the Ardennes–Rhenish Massif forms a slightly elevated region (up to 700 m). The relatively smooth surface envelope is formed by marine planation surfaces of Mesozoic and Palaeogene age (e.g. Demoulin, 1995a), which is dissected by several rivers, the most important being the Maas (Meuse) and Rhine rivers. From the age of the planation surfaces and the remains of Palaeocene and Late Cretaceous sediments, it is concluded that Tertiary uplift of the Ardennes started with large-scale tilting during Paleocene, after a very long period of tectonic quiescence during Mesozoic (Demoulin, 1995a). This was followed by a slight doming event during Eocene. The major doming of the Ardennes started during Late Oligocene and continued during Neogene and Quaternary. The river terraces indicate that uplift was accelerated during Middle Pleistocene (e.g. Van Balen et al., 2000).

Neogene and Quaternary uplift of the Ardennes–Rhenish Massif represents one of the best docu-

* Corresponding author.

E-mail address: gard@geo.vu.nl (D. Garcia-Castellanos).

0921-8181/00/$ - see front matter © 2000 Elsevier Science B.V. All rights reserved.
PII: S0921-8181(01)00058-3

mented cases of plateau uplift in the Northwestern European lithosphere. Following the first quantitative studies integrating different approaches in geology, geophysics and geochemistry in the early 1980s (Fuchs et al., 1983), more recently renewed attention has been focusing on the rates and the mechanisms of the processes forcing the interplay of tectonics and landform evolution in the area. These studies have benefited from new methodological and conceptual advances in different domains of earth sciences in the last 20 years. In particular, the increasing resolution in imaging crustal and upper mantle structures by deep seismic reflection profiling (Oncken et al., 1999) and seismic tomography (Bijwaard et al., 1998; Ritter et al., 2000) has provided new constraints on tectonic models for the polyphase evolution of the area. In addition, the seismic reflection data have provided the framework for the integration with neotectonic geomorphological and levelling studies carried out in the last few years (e.g. Demoulin, 1995b; Demoulin and Collignon, 2000; Van Balen et al., 2000). At the same time, seismotectonic studies and paleoseismological indications based on the results of trenching have documented a high level of intraplate seismicity in the area (Camelbeeck and Meghraoui, 1998).

However, fundamental questions still exist on the relationships between the deep-seated processes and the surface expressions of uplift. Whereas the data from the volcanic activity (Lippolt, 1983) and the recently obtained new seismic tomography data (Ritter et al., 2000) clearly point to the presence of localised deep-seated thermal anomalies under the Eifel region, the surface heat flow lacks a corresponding signature (Haenel, 1983). This is important as lithospheric basal heating has been inferred in previous works separately addressing the record of volcanism, uplift tectonics and seismic tomography (e.g. Fuchs et al., 1983). However, as pointed out by Haenel (1983), no heat flow signature of such a basal heating is observed, with typical heat flow values of 70 mW m^{-2}, characteristic for unperturbed Palaeozoic continental lithosphere. Drisler and Jacoby (1983) studied the gravity anomalies and density distribution pointing to a discrepancy between the velocity–density characteristics of both crust and upper mantle anomalies. This feature was interpreted by these authors in terms of the presence of fluid phases affecting both uplift and volcanism, in particular in their early stage.

This raises the question whether the thermal anomalies in the mantle have risen sufficiently high in the lithosphere to affect the thermal and mechanical structure of the overlying upper crust, at large. This is important as thermo-mechanical studies of the European lithosphere (Cloetingh and Burov, 1996) have revealed the presence of major intralithosphere decoupling levels, leading to a differential response of the upper crust and mantle lithosphere to intraplate tectonic processes (Ziegler et al., 1995, 1998). These authors have also drawn attention to the link between this spatial variation in bulk rheology of the European lithosphere, which is controlled by its thermo-tectonic age and compositional structure, and patterns in effective elastic thickness inferred from flexural foreland studies and depth distributions patterns of crustal seismicity (e.g. Cloetingh and Banda, 1992).

In the present paper, we follow a thermo-mechanical approach integrating the presently available data sets on surface uplift, seismicity distribution and crustal and upper mantle structure. The main innovative aspect of the present study is the quantification of the mechanical consequences of the inferred deep thermal anomaly below the Eifel region in terms of its weakening effect on the overlying lithosphere (see scheme in Fig. 1a).

The strategy we implement for this purpose consists of a number of steps depicted in Fig. 1b. In the first step, we calculate the lithospheric strength and the buoyant load distribution based on the thermal models by Goes et al. (2000a). Based on these results, we construct strength profiles representative for the perturbed (plume) area and the area not affected by deep-seated thermal processes. These yield stress envelopes are subsequently used to calculate the stress distribution in an elastic plastic plate induced by a buoyant load, corresponding to the deep-seated thermal anomaly, in a regional compressional intraplate tectonic context, representative for this segment of the Northwestern European lithosphere (Mueller et al., 1992). We use the outcome of this model to determine the magnitude and distribution of the equivalent elastic thickness of the lithosphere, which is used for the calculation of the flexural 2D (planform) deflection related to a deep

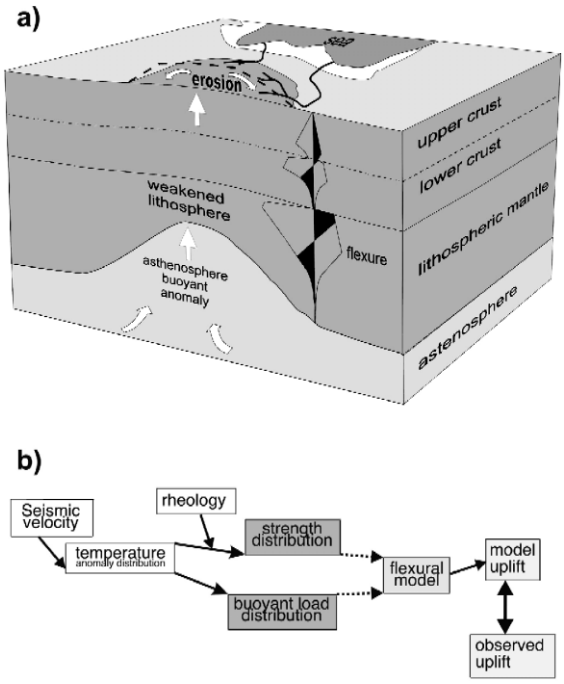


Fig. 1. Elements of the conceptual model (a) and strategy (b) adopted for this study.

buoyant load. Calculations are made with and without a lithospheric weakening, and the results are validated by the uplift data.

2. Uplift data

Over the last few years, a considerable body of observational constraints on the uplift of the Ardennes–Rhenish Massif has been accumulated as a result of river incision studies (Meyer and Stets, 1998; Van Balen et al., 2000), repeated levelling (Demoulin, 1995b), and GPS (Campbell and Kumpel, 1999).

Fig. 2 compiles the results of uplift studies by Meyer and Stets (1998) and Van Balen et al. (2000), based on incision of the Maas and Rhine rivers and their major tributaries. In the Ardennes–Rhenish Massif, the morphology of the river valley sections is characterised by a relatively flat and wide upper part with broad terrace surfaces, and a relatively narrow v-shaped lower part with narrow terrace surfaces. The transition of the wide valley to the narrow valley shape corresponds morphologically with the transition of the Main Terrace system to the Middle Terrace sequence and tectonically with a major increase in uplift rate of the Ardennes–Rhenish Massif. Because of the particular change in the morphology, the youngest Main Terrace can easily be identified and correlated over large areas. Based on paleomagnetic measurements, the youngest Main Terrace is inferred to be slightly younger than the Brunhes–Matayuma magnetic epoch boundary (Meyer and Stets, 1998; Van Balen et al., 2000), that is 0.78 Ma.

Using the documented river terrace stratigraphies, the vertical distance between the youngest Main Terrace and the present-day vertical position of the Maas and Rhine rivers is used to determine the incision of these rivers since 0.78 Ma. It is argued that this incision is primarily the response to tectonic uplift (Van Balen et al., 2000). As the Ardennes–Rhenish Massif is situated in the middle parts of the Maas and Rhine rivers, no corrections are made for the change in the shape of the equilibrium profiles of the rivers due to uplift of the upstream areas. It is assumed that in these middle reaches the equilibrium river profiles are approximately constant. However, for the tributary rivers that originate in the Ardennes–Rhenish Massif, such a correction is made (see Meyer and Stets, 1998; Van Balen et al., 2000). We refer to these authors for a full description of the methodology and the underlying data.

Here we focus on the Late Quaternary stage (younger than 780 ka) of uplift history. It should be noticed that these data do not necessarily correlate with present day uplift rates inferred from repeated levelling studies (Demoulin, 1995b), being also not perturbed by human effects like the uplift data sets studied by Klein et al. (1997). It is also important to note that the Late Quaternary and recent uplift was superimposed on pre-existent topography generated in Early Quaternary–Tertiary time in relation with the rifting in the Upper and Lower Rhine Graben systems during Eocene and Oligocene times, respectively, and with the Alpine foreland compression during Late Cretaceous and Eocene times (Ziegler, 1990).

The main trends of the uplift data (contoured in Fig. 2) show that the first-order pattern of uplift has a concentric symmetry around a point located between the Rhine and the Maas rivers. Another remarkable characteristic is the fact that the uplift

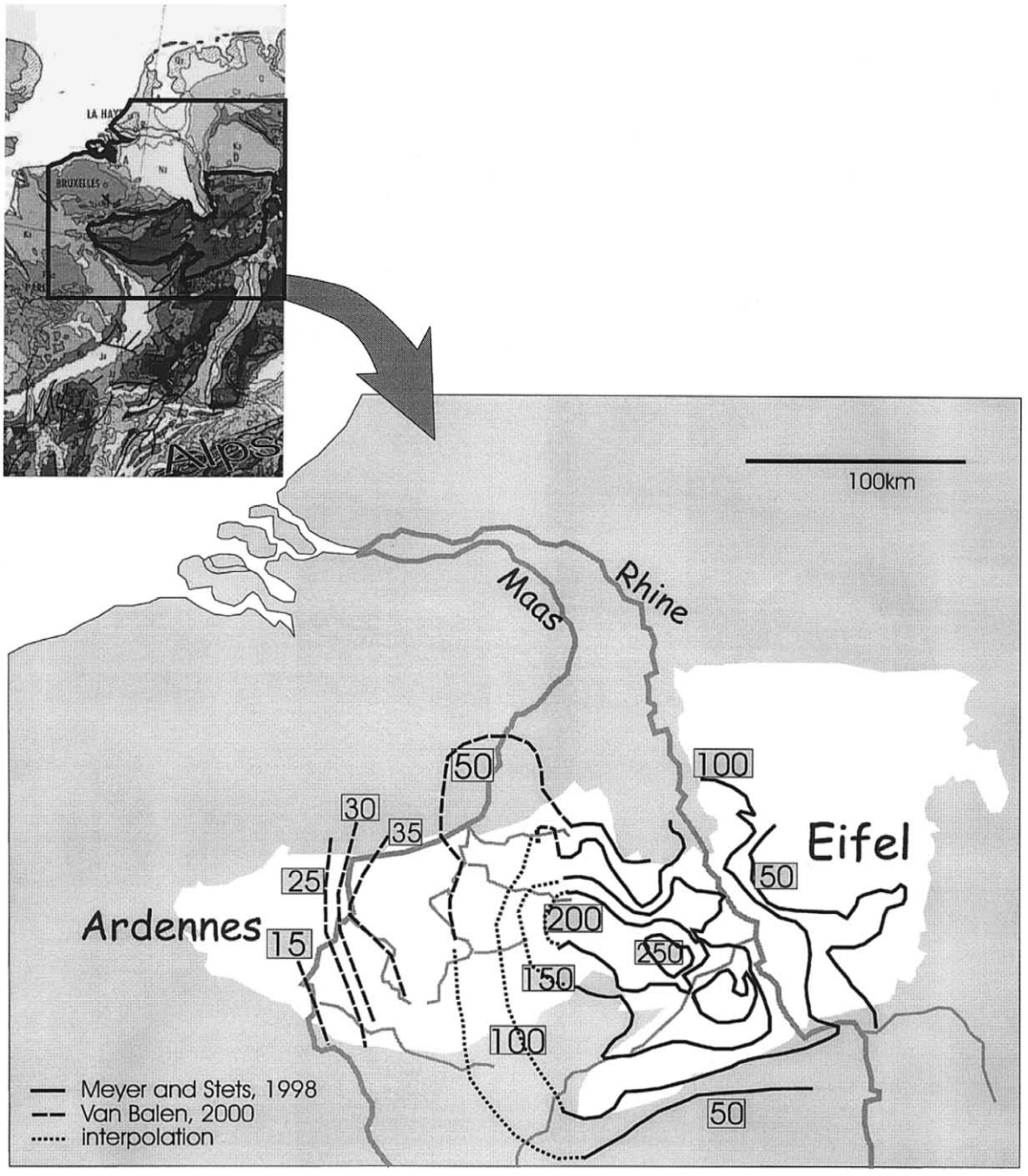


Fig. 2. Distribution of uplift during the last 800,000 years derived from a compilation of measures of river incision in the Ardennes and Rhenish Massif (labels in meters). Source data are from Meyer and Stets (1998) and Van Balen et al. (2000).

gradient increases towards the centre (maximum) of its distribution: the distance between the 15 and 35 m contours is comparable to that between the 100 and 200 m contours.

3. Constraints on the thermo-mechanical structure of the lithosphere

Lithospheric strength depends primarily on its compositional and thermal structure (Ranalli, 1987; Burov and Diament, 1995). In the construction of strength profiles, it has been common practice to use surface heatflow data (e.g. Cloetingh and Banda, 1992) or inferences from thermal modelling (e.g. Okaya et al., 1996a,b) to calculate the thermal input for the ductile part of the rheology. A novel and complementary approach is to use seismic velocity information for the calculation of lithospheric geotherms (e.g. Sobolev et al., 1996; Goes et al., 2000a,b). Based on studies of seismic tomography at European scale by Bijwaard et al. (1998), Goes et al (2000a) have reconstructed the present day thermal structure of the upper mantle below the continent. The uncertainty derived by these authors, related to the original uncertainty in the velocity field as a consequence of the tomography inversion and also to the conversion to temperature itself, is higher than 100–150°C for the upper mantle.

The temperatures derived by Goes et al. (2000a) from the seismic tomography of Bijwaard et al. (1998), provide an image of the lithosphere that is restricted to two horizontal surfaces at 52.5 and 90 km depth. Of primary concern in the present paper is the depth-dependent distribution of lithospheric strength as well as the thermal load acting on the lithosphere over the whole area affected by uplift. For this purpose, and to obtain a first-order estimate of the spatial distribution of the thermal load and its associated weakening, temperatures have been linearly interpolated between these two horizontal surfaces at 52.5 and 90 km depth. The resulting temperatures are then translated in terms of buoyant load in the mantle assuming a thermal expansion coefficient of mantle olivine of $\alpha = 3.0 \times 10^{-5}$ K^{-1}. Therefore, the resulting load distribution (Fig. 3a) is only constrained by temperature anomalies between 52.5 and 90 km. It should be noted that although the zero value of the inferred thermal load is arbitrary, the relative differences are of particular relevance to the uplift problem. The possible buoyant effect related to phase changes (i.e. partial melting), being probably a second order effect, is not taken into account. The distribution of lithospheric strength (Fig. 3b) is calculated using standard rheological parameter values (Lynch and Morgan, 1987) considering three layers for the lithosphere composition (quartzite, diorite and olivine). The earthquake location (extracted from the catalogue of the Council of the National Seismic System, USA) shows a family of earthquakes around the centre of uplift, all of which are located at crustal depths.

The calculated spatial distributions of the integrated buoyant load and the lithospheric strength do not coincide perfectly with the shape observed for the uplift (Figs. 2 and 3). Both the maximum load (40×10^6 N m^{-2}) and the minimum strength (2×10^{12} N m^{-2}) points are located out of the Rhenish Massif itself. Another misfit is the absence of a clear thermal anomaly under the Western Ardennes, whereas this area is marked by significant uplift with rates that underwent rapid acceleration during Late Quaternary time (Van Balen et al., 2000). This might be due to a number of factors, such as the uncertainty inherent to the original seismic tomography inversion and also the conversion from seismic velocity into temperature (Goes et al., 2000a). Furthermore, it is important to note that the period of uplift we study corresponds to a small fraction of the total duration of uplift that occurred since Eocene: changes in time of the location of the anomaly could lead to the situation in which its present position and the uplift do not perfectly coincide. At the same time, the spatial distribution of the seismicity clearly coincides with the main area of thermal mantle perturbation inferred from seismic tomography (Fig. 3b), suggesting a causal link between lithospheric neotectonic deformation and associated stress release and mantle upwelling. All this illustrates that both distributions displayed in Fig. 3 must be taken only as a reference for the subsequent thermo-mechanical modelling.

Based on the above considerations, two reference geotherms have been derived for the study area (Fig. 4). An unperturbed geotherm (representative for the areas surrounding the velocity anomaly) is based on a mean surface heat flow of 70 mW m^{-2} that connects in depth with the temperatures provided by Goes et al. (2000a,b). A perturbed strength envelope is calculated by connecting the same surface temperature gradient as in the unperturbed case with the anomalous temperatures by Goes et al. (2000a). A

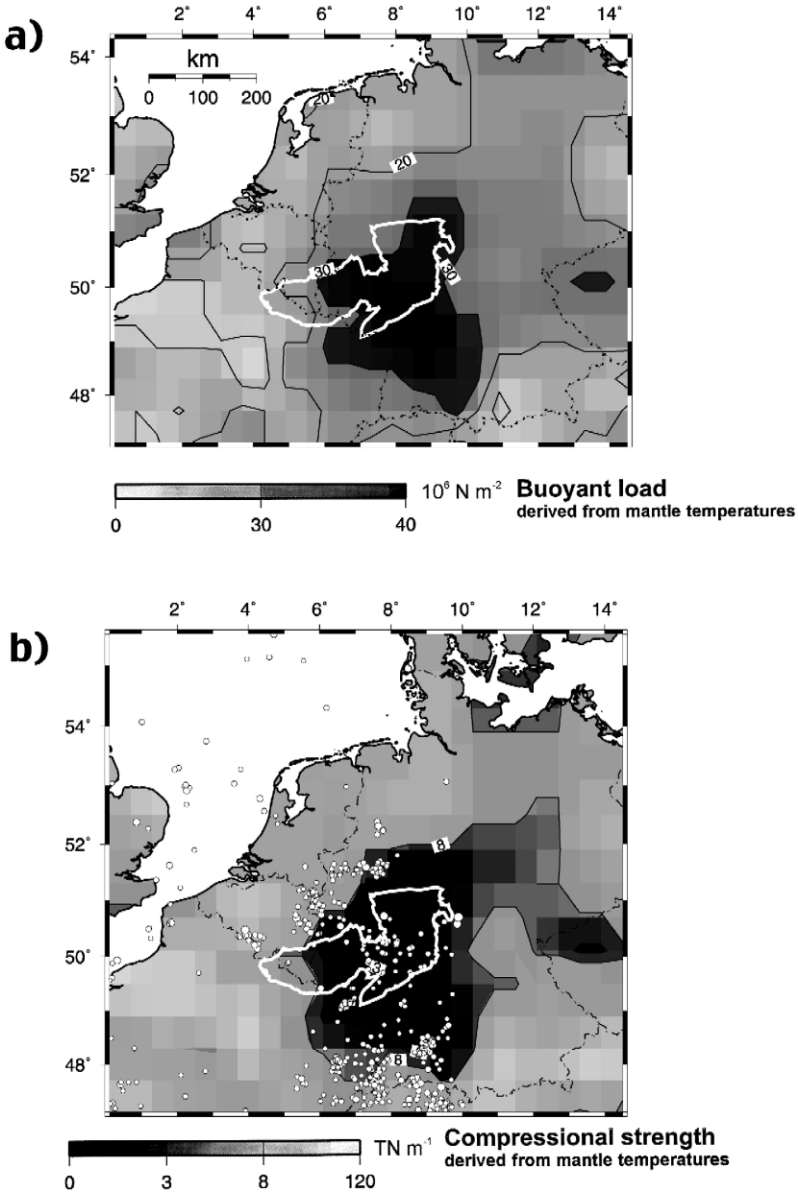


Fig. 3. Computed buoyant load (a) and integrated compressional strength (b) derived from the temperatures from Goes et al. (2000a). Contours are drawn every 10 MN/m^2 for the load. For the strength, the contours of 3 and 8 TN/m are plotted. Earthquake hypocenter distribution is also shown in (b).

strain rate of 10^{-16} s^{-1} is assumed for both strength envelopes. According to the strength profiles shown in Fig. 4, the integrated lithospheric strength is 2.2 TN m^{-1} under the Eifel and up to 21.0 TN m^{-1} in the adjacent areas, suggesting an order of magnitude difference in bulk strength. It is interesting to compare these strength profiles with the depth distribution of intraplate seismicity in the area. The earthquake hypocenter depth distribution compiled by Camelbeeck (1994) for the Ardennes/Hautes Fagnes area displays a bimodal distribution in the seismicity with a concentration in the upper and lower crust and

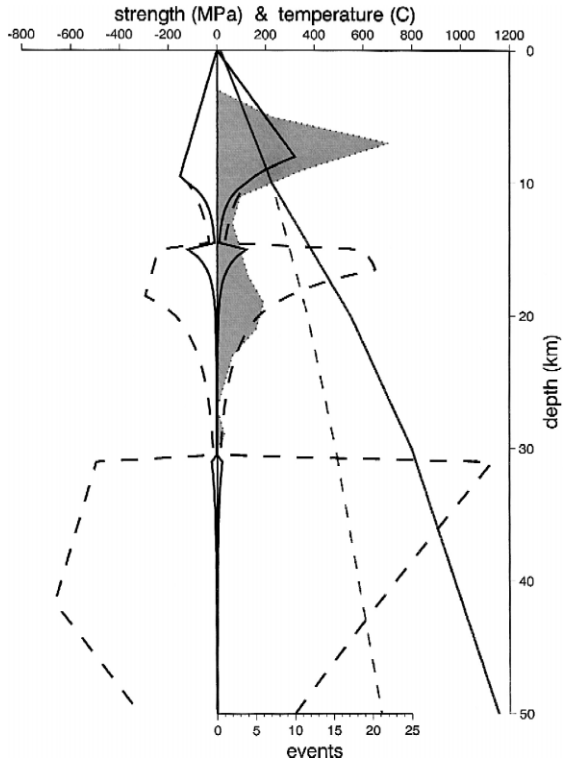


Fig. 4. Stress envelopes and geotherms constructed for the Eifel (continuous lines) and for the unperturbed surrounding areas (dashed lines). Dark shading shows the depth distribution of earthquakes under the Ardennes. Positive stresses mean compression.

a marked absence of seismicity in the upper mantle part of the lithosphere. This feature is in support of a mechanical decoupling between crust and upper mantle and/or localised weakening of upper mantle material.

4. Thermo-mechanical models for uplift: concepts and numerical implementation

4.1. Basic assumptions

The buoyant load and strength distributions obtained in the previous section demonstrate the combined effect of weakening and uplift related to the temperature anomaly. However, they are in themselves not reliable enough for the purpose of quantitatively explaining the uplift distribution. Therefore, we are in need of additional assumptions before trying to fit the uplift patterns.

It must be emphasised here that it is possible to fit any uplift distribution with a flexural model if the load generating it is not constrained a priori. In particular, a local isostasy approach (zero strength lithosphere, or $Te = 0$) and a load distribution proportional to the uplift at any given point, would perfectly fit the observations. However, this would be against the notions that (1) lithosphere is intrinsically characterised by finite strength when submitted to a tectonic load and (2) thermal buoyancy and weakening are linked processes that occur coeval in space. Both ideas have been extensively documented in the last decades. In particular, foreland basin analyses and studies of intraplate seismicity in the western European platform (see Cloetingh and Burov, 1996) point to the existence of non-zero equivalent elastic thickness, showing that the continent is far from a local isostatic equilibrium.

Hence, we will hereafter assume that both effects, load and weakening, although independent in magnitude, have the same spatial distribution. Varying arbitrarily their magnitudes will allow to constrain the presence of a lithospheric weakening related to the basal heating.

4.2. Implementation in numerical models

We have carried out a series of cross-sectional and planform modelling experiments. Our first numerical experiment consists of a 2D (cross-section) thin elasto-plastic plate that will allow to approach the stress distribution produced in the lithosphere during uplift. This numerical model of lithospheric flexure (similar to Burov and Diament, 1992) accounts for vertical and horizontal loads acting on a multilayered plate, the strength structure of which is a function of the crustal geometry, temperature, and rheological parameters, using the concept of yield stress envelope (YSE). A finite difference technique with a gridding of 600×120 is used. The numerical model is described in detail by Garcia-Castellanos et al. (1997) and has been applied to both continental and oceanic settings (Garcia-Castellanos, 1998; Garcia-Castellanos et al., 2000).

The main required inputs are the distributions of temperature and vertical load. As outputs, the model

provides the uplift profile (deflection) and a stress distribution being directly consistent with the YSE lateral variations. A subproduct of the model is the lateral variation of effective elastic thickness, which is computed as a function of strength and plate curvature (Burov and Diament, 1992).

Since the process we study is far from a 2D (cross-section) approach, it is required a planform flexural model in order to fit the uplift distribution. The model consists of a pure elastic thin plate allowing for lateral variations of elastic thickness, which are related to the plate rigidity and is the main model input together with the load distribution. The differential equations involved are taken from Van Wees and Cloetingh (1994) and solved using the finite difference method using an 80×80 nodes mesh. The role of plate curvature during lithospheric flexure discussed by Burov and Diament (1992, 1995) is not incorporated in this model because the relative small amount of deflection (uplift) in this area is insufficient to produce relevant reductions of rigidity.

5. Results

The coincident distribution of load and weakening is assumed to be truncated cone-shaped (trapezium for the cross-section model). In all results shown

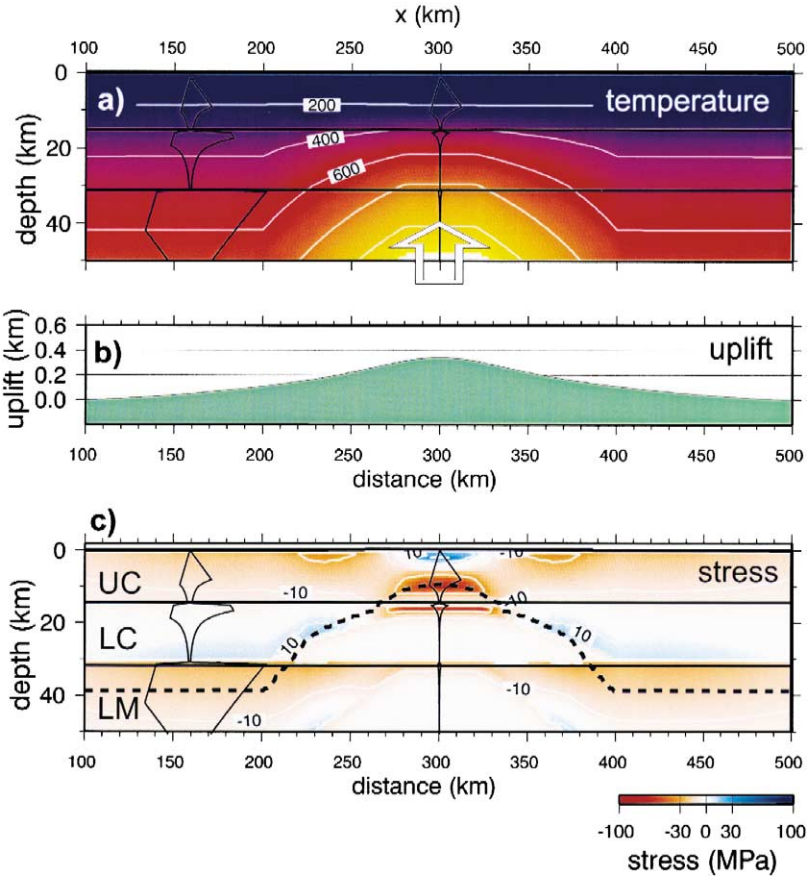


Fig. 5. 2D elastic plastic plate synthetic model. Input temperatures (above), uplift distribution (middle panel) and stress distribution (lower panel) predicted in the model assuming a low compression regional setting ($F_x = 1$ TN/m). Positive stresses (in blue) mean extension. The black lines show the strength profiles (YSE) representative for both the unperturbed and the anomalous zones. The dashed line is the predicted elastic thickness. UC: upper crust; LC: lower crust; LM: lithospheric mantle. Bold lines indicate the base of the Upper and Lower Crust.

here, the dimensions of the load are 200 km (base diameter where load and weakening are zero) and 40 km (top diameter), based on the results shown in Fig. 3. Different values of the distribution width were tested but, although this parameter influences the shape of the deflection, it does not affect the general conclusions obtained in this work.

5.1. Cross-section synthetic model

Fig. 5 displays the results of loading the cross-section model with a vertical buoyant load in a horizontal compressional regime.

The temperatures used as input, shown in Fig. 5a, are based on a steady state hypothesis using a surface heat flow of 70 mW m^{-2} (Haenel, 1983), except for the areas affected by heating, for which we use the temperatures by Goes et al. (2000a) as a constraint for the mantle. A constant crustal thickness of 31 km is adopted. Both the anomalous temperatures and the load have a distribution shaped as a truncated triangle the base and top of which are between $x = 200$ and 400 km and between $x = 280$ and 320 km, respectively. Maximum load (in the centre) is arbitrarily set to 13.2×10^6 N m^{-2} (equivalent to a 27-km-thick body with a buoyant density

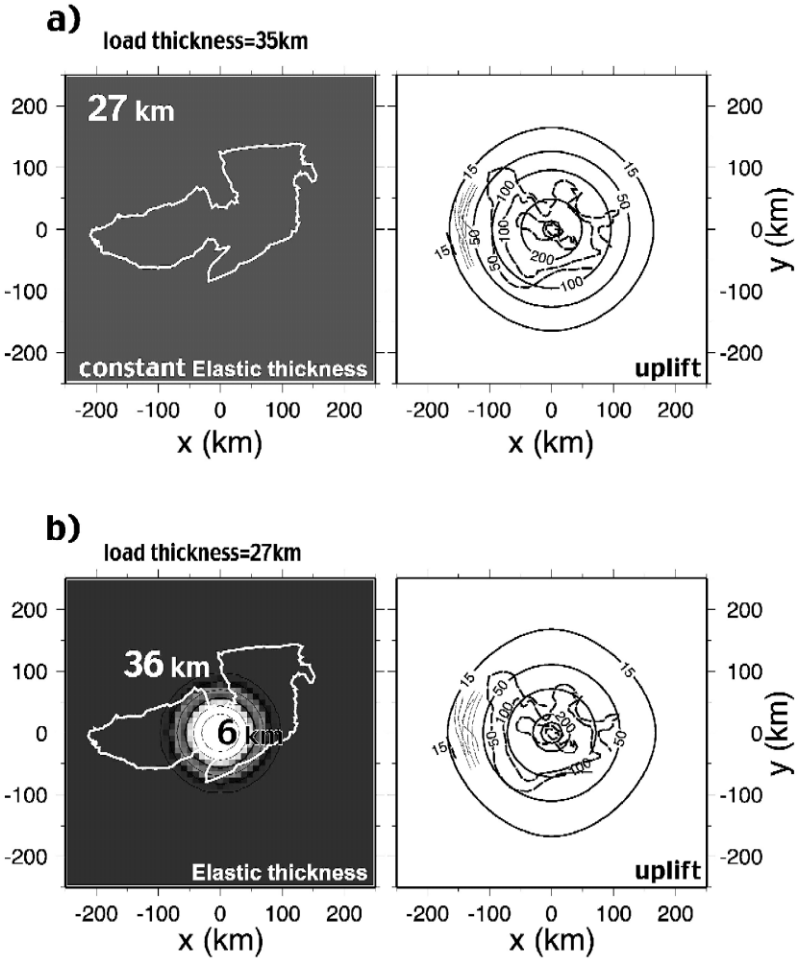


Fig. 6. Elastic thickness planform distribution (left) and best fits of the uplift distribution (right) using a 2D (planform) flexural elastic plate for the case of constant elastic thickness (a) and laterally varying elastic thickness (b). The thicker isolines of observed (dashed) and calculated (continuous) uplift correspond to 15, 50, 100, 200, 250 m. The thin lines correspond to 25, 30, 35 and 150 m. The white line indicates the contour of the Ardennes–Rhenish Massif basement outcrop.

contrast of 50 kg m^{-3}). This load predicts a fairly realistic uplift pattern with a maximum value of 384 m. This overestimation of the observed uplift is to a large extent due to the 2D limitation of the model.

The predicted uplift (Fig. 5b) does not depend substantially on the applied horizontal force (1 TN m^{-1} in this model) even despite the applied force is comparable with the plate strength. It is interesting, however, that the stress predicted on top of the anomaly (Fig. 5c) is extensional despite the assumption of a regional compressional regime. This is in agreement with the extensional stresses observed in the central Eifel (Bauman and Illies, 1983; Mueller et al., 1997) in spite of the compressional context of central Europe. The extensional stress is the result of the upward bending at the upper part of the crust due to the uplift. The model also predicts the equivalent elastic thickness variations, showing a decrease from 39 km in the unperturbed areas to less than 10 km in the central part. This reduction is due both to the thermal weakening and the flexural plate curvature. These values will be used as an additional constraint for the planform modelling.

5.2. Planform modelling

Fig. 6 shows the best fits of the uplift observations with a 2D planform flexural model. Two cases were studied: constant elastic thickness and lateral varying elastic thickness. In the previous experiment, the lithospheric weakening has been assumed to coincide in space with the load. In order to reproduce the general trends of the uplift distribution, we use a thin 2D elastic plate with variable thickness to simulate the deflection of the lithosphere. The load distribution is shaped as a truncated cone, with a maximum radius of 100 km, where the load is zero, and a minimum radius of 20 km, where the load is maximum. This agrees with the characteristic wavelength of lithospheric thinning in the Rhenish Massif derived by Neugebauer et al. (1983): between 100 and 200 km.

The best fit with a constant elastic thickness is obtained for a load of 17.2×10^6 N m^{-2} (maximum value), equivalent to a 35-km-thick buoyant body of 50 kg m^{-3} of contrast density. Whereas elastic thickness affects the lateral extension of the flexural uplift, the magnitude of the load modifies primarily the magnitude of the deflection. Although the predicted uplift fits satisfactorily the maximum and minimum constrained isolines (15 and 250 m), the zone in between them is not satisfactorily fitted, as shown by the 50- and 100-m isolines.

Instead, accounting for a plate thickness reduction (Fig. 6b) restricted to the same area as the load, the fit is acceptable for all the constrained isolines. This property has been checked with different load and weakening magnitudes. The load required for this model was 13.2×10^6 N m^{-2} (maximum value), equivalent to a 27-km-thick buoyant body of 50 kg m^{-3} of contrast density.

6. Discussion: thermal weakening and lithosphere memory during uplift localisation

The modelling results demonstrate that the shape of the uplift distribution can be explained as the response to buoyant loading of a hot subcrustal body, and to the associated mechanical lithospheric weakening.

The model proposed here, based on flexural response of the lithosphere to the buoyant load, is fundamentally constrained by the uplift distribution. At the same time, it is however also consistent with the existence of extensional stresses that are measured near the surface of the Rhenish Massif (Bauman and Illies, 1983) probably dominating over the superimposed regional compressional plate-wide stress field in Northwest Europe.

More accurate seismic tomography (Ritter et al., 2000), together with new measurements of river incision, is important to further constrain and validate the models. At present, it appears that short wavelength discrepancies between model and observed uplift can be related to other factors such as fault reactivation and the sediment loading in the surrounding graben areas (see e.g. Houtgast and van Balen, 2000; Dirkzwager et al., 2000).

Although the lithospheric weakening inferred here has been implicitly linked to a thermal anomaly, the role of other phenomena cannot be dismissed. One of these factors could be weakening induced by pre-existent fault structures, and the effect of superimposed compression acting on such weakness zones leading intrinsically to further concentration of localised de-

formation. In this context, it should be noted that in the Northwestern European lithosphere, the effect of compression on vertical motions has been shown to be of great significance in the area adjacent to the Ardennes–Eifel area, including the Paris Basin and the North Sea area (Cloetingh et al., 1999; Van Balen et al., 1998; Van Wees and Cloetingh, 1996). In future work, it will be of particular importance to obtain better constraints on the fine structure of the spatial and temporal variations in the interplay of thermal perturbations and stresses on the full depth range of the mechanically strong part of the lithosphere.

The gravity signal of the buoyant body derived in this work is not clearly reflected in the Bouguer anomaly distribution (Drisler and Jacoby, 1983; Lee et al., 1993), which indeed shows relevant asymmetry in the domain of the Rhenish Massif (Jacoby et al., 1983). Simple calculations show that the gravity anomaly associated with the geometry derived here for the anomalous body ($\Delta\rho = 50$ kg m^{-3}) would produce a maximum anomaly lesser than 25 mGal, decreasing to less than 10 mGal at a 100-km distance from the centre of the body. This relatively small anomaly with smooth lateral variation (related to the deep location of the body, in the lithospheric mantle) may have been overprinted by the gravity effect of other mechanisms, such as inherited heterogeneity in the crustal structure and/or the subregional character of the mantle diapirism related with the buoyant body (Neugebauer et al., 1983), which could be co-responsible for the complicated pattern of the gravity anomaly.

Recently, it has been shown that asthenospheric diapirism can be initiated by rifting processes (Huismans, 1999): thinning of the lithosphere creates a topography at the lithosphere–asthenosphere boundary, which induces further upwelling of low density asthenosphere, resulting in uplift at the surface. In such a model, active rifting is the consequence of passive rifting. The model predicts that a few million years after a rifting phase, the basin and its immediate surroundings are uplifted. This might be applicable to the Ardennes–Rhenish Massif, which is dissected by Tertiary rift-systems. The Middle Pleistocene uplift of the area could be a response to this mode of secondary asthenospheric diapirism.

A further quantification of the erosion-driven isostatic forcing of uplift is also an important future goal. The removal of crustal mass by erosion affects

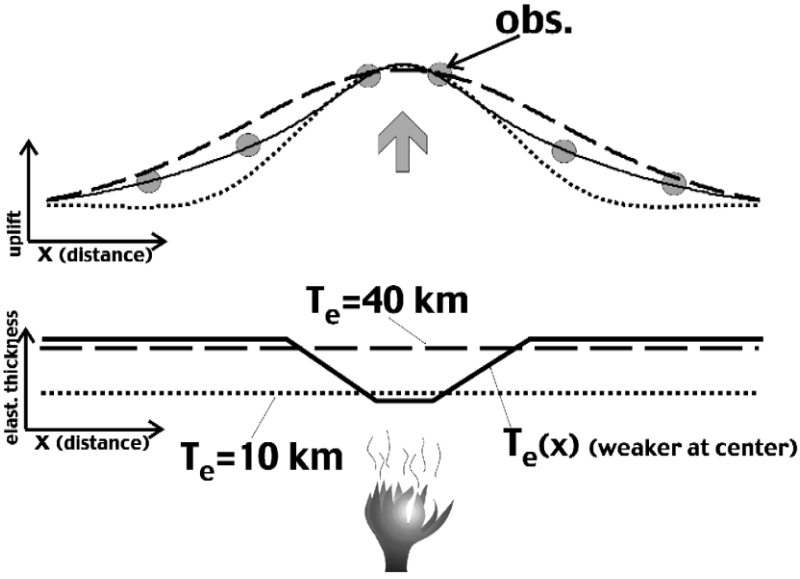


Fig. 7. Cartoon illustrating in a vertical cross-section the necessity for a lithospheric weakening in the flexural model. A plate with constant elastic thickness (dashed and dotted lines) can fit the maximum and minimum uplift observations. A model with lateral variations of elastic thickness (bold lines) allows fitting the intermediate values.

the load distribution on the asthenosphere and lower crust, which might lead to flow of mantle and lower crustal rocks, respectively (Burov and Cloetingh, 1997), thereby causing vertical motions at the surface.

An important outcome of our models is the prediction of strong lateral variations in the mechanical structure in the uplifted area. It appears that models with uniform elastic thickness fail to explain observed patterns of uplift. It should be noted that this finding is important in terms of future observational studies of the uplift. Although the magnitude of the buoyant load as main generator of uplift is poorly constrained (Fig. 3), we are still able to distinguish the effect of a localised weakening. Inspection of Fig. 7 illustrates that accounting for a weakening coincident in space with the buoyant load allows to increase the gradient of uplift towards the centre of its distribution, as observed in the study region. However, our results do not allow to discriminate whether this weakening is exclusively related to the thermal perturbation or it is to some extent related to pre-existing structures.

The low values of elastic thickness that have been obtained (down to 6–10 km under the Eifel) and the strength profiles indicate that the crust and the lithospheric mantle may be mechanically decoupled in the region. The high value (close to 40 km) in the area unaffected by heat and curvature is consistent with flexural studies in the western European platform (Cloetingh and Burov, 1996; Andeweg and Cloetingh, 1998).

7. Conclusion

Our analysis has shown that the large scale pattern of the Late Quaternary uplift of the Ardennes–Rhenish Massif region can be explained in terms of a flexural response of the lithosphere to a buoyant subcrustal load. A localised plate weakening coeval in space with the action of the buoyant load predicts an uplift, which is in better agreement with the observations than considering an homogeneous distribution of lithosphere rigidity. This spatial coexistence of load and weakening points to a primary control by thermo-mechanical processes at deeper lithospheric levels. This weakening might be amplified by reactivation of inherited fault structures at shallower levels.

Acknowledgements

We gratefully acknowledge the corrections and comments of the reviewers Marcus Schumacher, Evgenii Burov and Andreas Petereck. This study was carried out as part of the Netherlands Environmental Earth System Dynamics Initiative (NEESDI) funded by the Netherlands Organisation of Scientific Research NWO. Saskia Goes kindly provided the mantle temperatures. This is NSG contribution 2000-0503.

References

Andeweg, B., Cloetingh, S., 1998. Flexure and unflexure of the North Alpine German–Austrian Molasse Basin: constraints from forward tectonic modelling. In: Mascle, A., Puigdefabregas, C., Luterbacher, H., Fernandez, M. (Eds.), Cenozoic Foreland Basins of Western Europe. Geological Society of London Special Publications, vol. 134, pp. 403–422.

Bauman, H., Illies, H., 1983. Stress field and strain release in the Rhenish Massif. In: Fuchs (Ed.), Plateau Uplift: The Rhenish Shield, A Case History. Springer-Verlag, Berlin, pp. 177–186.

Bijwaard, H., Spackman, W., Engdahl, E.R. et al., 1998. Closing the gap between regional and global travel time tomography. J. Geophys. Res. 103, 30055–30078.

Burov, E.B., Diament, M., 1992. Flexure of the continental lithosphere with multilayered rheology. Geophys. J. Int. 109, 449–468.

Burov, E.B., Diament, M., 1995. The effective elastic thickness (Te) of continental lithosphere: what does it really mean? J. Geophys. Res. 100, 3905–3927.

Burov, E., Cloetingh, S., 1997. Erosion and rift dynamics; new thermomechanical aspects of post-rift evolution of extensional basins. Earth Planet. Sci. Lett. 150 (1–2), 7–26.

Camelbeeck, T., 1994. Mecanisme au foyer des tremblements de terre et contraintes tectoniques: le cas de la zone intraplaque belge. PhD Thesis. Universite Catholique de Louvain. Bruxelles, 1994.

Camelbeeck, T., Meghraoui, M., 1998. Geological and geophysical evidence for large palaeo-earthquakes with surface faulting in the Roer Graben (Northwest Europe). Geophys. J. Int. 132, 347–362.

Campbell, J., Kumpel, H.-J., 1999. Recent movement pattern of the lower Rhine Basin from GPS data. Workshop SFB350: Rift tectonics and synergetic Sedimentation—the Cenozoic Lower Rhine graben and related structures. Universitaet von Bonn, November 1999.

Cloetingh, S., Banda, E., 1992. Europe's lithosphere; physical properties; mechanical structure. In: Blundell (Ed.), A Continent Revealed: The European Geotraverse. Cambridge Univ. Press, Cambridge, UK, pp. 80–91.

Cloetingh, S., Burov, E. et al., 1996. Thermomechanical structure of European continental lithosphere: constraints from rheological profiles and EET estimates. Geophys. J. Int. 124, 695–723.

Cloetingh, S., Burov, E., Poliakov, A., 1999. Lithospheric folding: primary response to compression? (from central Asia to Paris Basin). Tectonics 18, 1064–1083.

Demoulin, A., 1995a. L'Ardenne des Plateaux, heritage des temps anciens-surfaces d'erosion en Ardenne. In: Demoulin, A. (Ed.), L'Ardenne, essai de géografie physique. Dep. Géogr. Phys. Quat., Univ. Liège, pp. 68–93.

Demoulin, A., 1995b. L'Ardenne bouge toujours-neotectonique du massif Ardennais. In: Demoulin, A. (Ed.), L'Ardenne, essai de géografie physique. Dep. Géogr. Phys. Quat., Univ. Liège, pp. 110–135.

Demoulin, A., Collignon, A., 2000. Nature of the recent vertical ground movements inferred from high-precision leveling data in an intraplate setting: NE Ardenne, Belgium. J. Geophys. Res. 105 (B1), 693–705.

Dirkzwager, J.B., van Wees, J.D., Cloetingh, S.A.P.L., Geluk, M.C., Dost, B., Beekman, F., 2000. Geo-mechanical and rheological modelling of upper crustal faults and their near-surface expression in The Netherlands. Global Planet. Change 27, 67–88.

Drisler, J., Jacoby, W., 1983. Gravity anomaly and density distribution of the Rhenish Massif. In: Fuchs (Ed.), Plateau Uplift: The Rhenish Shield, A Case History. Springer-Verlag, Berlin, pp. 366–380.

Fuchs, K., von Gehlen, K., Malzer, H., Murawski, H., Semmel, A. (Eds.), 1983. Plateau Uplift: The Rhenish Shield, A Case History. Springer-Verlag, Berlin, 411 pp.

Garcia-Castellanos, D., 1998. Desarrollo de modelos numéricos de flexion litosférica. Aplicación de cuencas de antepaís y fosas oceánicas. PhD thesis, Universitat de Barcelona, 1998.

Garcia-Castellanos, D., Fernàndez, M., Torné, M. et al., 1997. Numerical modeling of foreland basin formation: a program relating thrusting, flexure, sediment geometry and lithosphere rheology. Comput. Geosci. 23 (9), 993–1003.

Garcia-Castellanos, D., Torné, M., Fernàndez, M., 2000. Slab pull effects from a flexural analysis of the Tonga and Kermadec Trenches (Pacific Plate). Geophys. J. Int. 141, 479–485.

Goes, S., Govers, R., Vacher, P., 2000a. Shallow mantle temperatures under europe from P and S wave tomography. J. Geophys. Res. 105 (B5), 11153–11169.

Goes, S., Loohuis, J.J.P., Wortel, M.J.R., Govers, R., 2000b. The effect of plate stresses and shallow mantle temperatures on tectonics of northwestern Europe. Global Planet. Change 27, 23–38.

Haenel, 1983. Geothermal investigations in the Rhenish Shield. In: Fuchs (Ed.), Plateau Uplift: The Rhenish Shield, A Case History. Springer-Verlag, Berlin, pp. 228–247.

Houtgast, R.F., van Balen, R.T. et al., 2000. Neotectonics of the Roer Valley Rift System, The Netherlands. Global Planet. Change 27, 131–146.

Huismans, R., 1999. Dynamic Modelling of the transition from passive to active rifting, Application to the Pannonian Basin. PhD Thesis. Vrije Universiteit, Amsterdam, The Netherlands.

Jacoby, W., Joachimi, H., Gerstenecker, C., 1983. The gravity field of the Rhenish Massif. In: Fuchs (Ed.), Plateau Uplift: The Rhenish Shield, A Case History. Springer-Verlag, Berlin, pp. 247–258.

Klein, A., Jacoby, W., Smilde, P. et al., 1997. Mining-induced crustal deformation in north-western Germany: modelling the rheological structure of the lithosphere. Earth Planet. Sci. Lett. 147, 107–123.

Lee, M.K., Pharaoh, T.C., Williamson, J.P., Green, C.A., de Vos, W., 1993. Evidence on the deep structure of the Anglo–Brabant Massif from gravity and magnetic data. Geol. Mag. 130 (5), 575–582.

Lippolt, H.J., 1983. Distribution of volcanic activity in space and time. In: Fuchs (Ed.), Plateau Uplift: The Rhenish Shield, A Case History. Springer-Verlag, Berlin, pp. 112–121.

Lynch, H.D., Morgan, P. et al., 1987. The tensile strength of the lithosphere and the localization of extension. In: Coward, M.P., Dewey, J.F., Hanock, P.L. (Eds.), Continental Extension Tectonics. Geol. Soc., Spec. Publ., vol. 28, pp. 53–65.

Meyer, W., Stets, J., 1998. Junge Tektonik im Rheinischen Schiefergebirge und ihre Quantifizierung. Z. Dtsch. Geol. Ges. 149, 359–379.

Mueller, B., Zoback, M.L., Fuchs, K., Mastin, L., Gregersen, S., Pavoni, N., Stephanson, O., Ljunggren, C., 1992. Regional patterns of tectonic stress in Europe. J. Geophys. Res. 97, 11783–11803.

Mueller, B., Wehrle, V., Fuchs, K., 1997: The 1997 release of the World Stress Map (available on-line at http://www-wsm.physik.uni-karlsruhe.de/pub/Rel97/wsm97.html).

Neugebauer, H.J., Woidt, W.-D., Wallner, H., 1983. Uplift, volcanism and tectonics: evidence for mantle diapirs at the Rhenish Massif. In: Fuchs (Ed.), Plateau Uplift: The Rhenish Shield, A Case History. Springer-Verlag, Berlin, pp. 381–403.

Okaya, N., Freeman, R., Kissling, E., Mueller, S. et al., 1996a. A lithospheric cross-section through the Swiss Alps: I. Thermokinematic modelling of the Neoalpine orogeny. Geophys. J. Int. 125 (2), 504–518.

Okaya, N., Cloetingh, S., Mueller, S., 1996b. A lithospheric cross-section through the Swiss Alps: II. Constraints on the mechanical structure of a continent–continent collision zone. Geophys. J. Int. 127 (2), 399–414.

Oncken, O., von Winterfeld, C., Dittmar, U., 1999. Accretion of a rifted passive margin: the late Paleozoic Rhenohercynian fold and thrust belt (middle European Variscides). Tectonics 18, 75–91.

Ranalli, G., 1987. Rheology of the Earth. Allen and Unwin, Boston, 366 pp.

Ritter, J.R.R., Achauer, U., Christensen, U.R., Eifel Plume Team, 2000. The teleseismic tomography experiment in the Eifel region, Central Europe: design and first results. Seismol. Res. Lett. 71 (4), 437–443.

Sobolev, S.V., Zeyen, H., Stoll, G., Werling, F., Altherr, R., Fuchs, K., 1996. Upper mantle temperatures from teleseismic tomography of French Massif Central including effects of

composition, mineral reactions, anharmonicity, anelasticity and partial melt. Earth Planet. Sci. Lett. 139, 147–163.

Van Balen, R.T., Podladchikov, Yu.Yu., Cloetingh, S.A.P.L., 1998. A new multi-layered model for intraplate stress-induced differential subsidence of faulted lithosphere, applied to rifted basins. Tectonics 17, 938–954.

Van Balen, R.T., Houtgast, R.F., Van der Wateren, F.M., Vandenberghe, J., P.W., Bogaart, 2000. Sediment budget and tectonic evolution of the Maas catchment in the Ardennes and the Roer Valley Rift System. Global Planet. Change 27, 113–129.

Van Wees, J.D., Cloetingh, S., 1994. A finite-difference technique to incorporate spatial variations in rigidity and planar faults into 3-D models for lithospheric flexure. Geophys. J. Int. 117, 179–195.

Van Wees, J.D., Cloetingh, S., 1996. 3D flexure and intraplate compression in the North Sea basin. In: Cloetingh, S., Ben-Avraham, Z., Sassi, N., Horvath, F. (Eds.), Dynamics of Extensional Basins and Inversion Tectonics. Tectonophysics, 266, pp. 343–359.

Ziegler, P., 1990. Collision related intra-plate compression deformation in Western and Central Europe. J. Geodyn. 11 (4), 357–388.

Ziegler, P.A., Cloetingh, S., Van Wees, J.D., 1995. Dynamics of intra-plate compressional deformation: the alpine foreland and other examples. Tectonophysics 252, 7–59.

Ziegler, P.A., Van Wees, J.D., Cloetingh, S., 1998. Mechanical controls on collision-related compressional intraplate deformation. Tectonophysics 300, 103–129.